

A&A manuscript no.
(will be inserted by hand later)

Your thesaurus codes are:
2(02.03.1), 03.13.4, 05.03.1

ASTRONOMY
AND
ASTROPHYSICS

The power spectrum of geodesic divergences as an early detector of chaotic motion

Ch.L. Vozikis, H. Varvoglis and K. Tsiganis

Aristotle University of Thessaloniki, Department of Physics, Section of Astrophysics, Astronomy and Mechanics,
54006 Thessaloniki, Greece

Received, 1999 / Accepted, 2000

Abstract. We propose a new method for determining the stochastic or ordered nature of trajectories in non-integrable Hamiltonian dynamical systems. The method consists of constructing a time-series from the divergence of nearby trajectories and then performing a power spectrum analysis of the series. Ordered trajectories present a spectrum that consists of a few spikes while the spectrum of stochastic trajectories is continuous. A test of the method with three different systems, a 2-D mapping as well as a 2-D and a 3-D Hamiltonian, shows that the method is fast and efficient, even in the case of sticky trajectories. The method is also applied to the motion of asteroids in the Solar System.

Key words: Chaos – Methods: numerical – Celestial Mechanics, stellar dynamics

1. Introduction

The problem of distinguishing a chaotic from an ordered trajectory in a non-integrable Hamiltonian system has been a topic of active investigation since the pioneering work of Hénon and Heiles (1964). Initially, when the study was restricted to 2-D systems, the work was done through surface of section plots. Later, when systems with more than 2-D were considered, the method of choice was the calculation of the Lyapunov Characteristic Numbers (LCNs) (Benettin et al. 1976, Froeschlé 1984). Unfortunately both the above methods suffer from the same drawback, namely they are not able to distinguish easily an ordered from a “sticky” chaotic trajectory. Various methods have been devised since then to address the above problem, namely the distinction of an ordered from a chaotic trajectory using a relatively short-time trajectory segment.

These methods generally fall into two main classes: those that use frequency or correlation analysis of a time-series, constructed by the values of generalized co-ordinates (or functions of them), and those that use the geodesic divergence of initially nearby trajectories. In the first class belong the “old” method of the rotation number (Contopoulos 1966), the frequency map

analysis developed by Laskar (Laskar et al. 1992, Laskar 1993) and the power spectrum analysis of quasi-integrals developed by Voyatzis & Ichtiaroglou (1992). In the second belong the probability density function analysis of stretching numbers developed by Froeschlé et al. (1993) and Voglis & Contopoulos (1994) and the Fast Lyapunov Indicators method developed by Froeschlé et al. (1997). Each one of the above methods has its own advantages and weaknesses; in particular some of them are more suitable to test *large sets of trajectories* rather than *single ones*, some are more efficient for *2-D systems* rather than for *$N(>2)$ -D systems* and some perform better for *mappings* rather than *flows*.

In 1997, Contopoulos & Voglis introduced a new method for distinguishing chaotic from ordered trajectories, which does not belong to any of the above mentioned two classes but, instead, may be classified as “mixed”. This new method is based on the analysis of the probability density of *helicity* and *twist angles*. Voglis & Efthymiopoulos (1998) and subsequently Froeschlé & Lega (1998) showed that the twist angles method is very efficient in testing *phase space regions*, at least in cases of 2-D systems, where the twist angles can be easily calculated. More recently Voglis et al. (1998, 1999) proposed two new and very efficient methods, namely the method of “Dynamical Spectral Distance” (DSD), which is particularly suitable for the characterization of single trajectories in 4-D maps, and the method of “Rotational Tori Recognizer” (ROTOR) which is very efficient for testing wide areas of the phase space of 2-D maps.

In the present paper we are introducing a new “mixed” method, which we show that it is at least as sensitive as the other methods in the literature, may be applied in a straightforward way to dynamical systems with more than two degrees of freedom and is equally efficient for single trajectories as well as large sets of them. The method consists in analyzing a time series constructed by the values of the geodesic deviation of nearby trajectories recorded at a properly selected frequency. It should be noted that a method based on a similar technique has been proposed by Lohinger and Froeschlé (1993).

The paper is organized as follows. Section 2 describes the basic features of the method, which, in Section 3, is tested upon three dynamical systems of different types. A comparison of the results of our method to those derived by various other

Send offprint requests to: Ch.L. Vozikis

Correspondence to: chriss@astro.auth.gr

methods is made in Section 4. Section 5 treats the application of the proposed method to one of the most important problems of solar system dynamics, the motion of asteroids. Finally in Section 6 we present our conclusions.

2. The method

In order to decide on the nature of a trajectory (chaotic or not), we work as follows. We integrate numerically the “main” trajectory together with a nearby one, which at a time $t_0 = 0$ starts at an infinitesimal distance in phase space, d_0 , from the main, and we calculate their distance, d_1 , at a time $t = t_0 + \Delta t$. Let us denote by q the logarithm of the ratio of the two distances, $q = \ln(d_1/d_0)$. We then renormalize the nearby trajectory, so as to start from a new position in phase space, which is at distance d_0 from the main trajectory in the direction of d_1 . The trajectories are followed once again for a time interval Δt and a new q is calculated. After following the trajectories for a time interval $T = N \Delta t$, we have constructed a time series consisting of the consecutive q ’s

$$q(t) = \ln \left[\frac{d_t}{d_0} \right] \quad \text{or} \quad q_k = \ln \left[\frac{d_k}{d_0} \right]_{t_k} \quad (1)$$

An ordered trajectory of a N-D conservative dynamical system will lie on an invariant torus, i.e. a N-D manifold of the 2N-D phase space. Any such trajectory is, in general, quasi-periodic and covers densely the invariant set. If a nearby trajectory is started at an infinitesimal distance from the previous one, this too would, in general, lie on an invariant torus, so that the $q(t)$ time series should behave in a quasi-periodic manner. On the other hand, a chaotic trajectory visits different regions of phase space in a stochastic manner and $q(t)$ should also be “random”.

Following the above considerations we calculate the *power spectrum* $P(f)$ of the $q(t)$ time series. We first calculate the discrete Fourier transform of the q_k multiplied by a *window function* w_k

$$Q_j = \sum_{k=0}^{N-1} q_k w_k e^{2\pi i j k / N} \quad j = 0..N-1 \quad (2)$$

Then the power spectrum, $P(f)$, is defined in $M = N/2 + 1$ frequencies as

$$\begin{aligned} P(f_0) &= \frac{1}{W} |Q_0|^2 \\ P(f_j) &= \frac{1}{W} (|Q_j|^2 + |Q_{N-j}|^2) \quad j = 1..(\frac{N}{2} - 1) \\ P(f_c) &= \frac{1}{W} |Q_{N/2}|^2 \end{aligned} \quad (3)$$

where

$$W = N \sum_{k=0}^{N-1} w_k^2 \quad (4)$$

and $f_c = f_{N/2}$ is the Nyquist frequency defined as

$$f_c = \frac{1}{2\Delta t}. \quad (5)$$

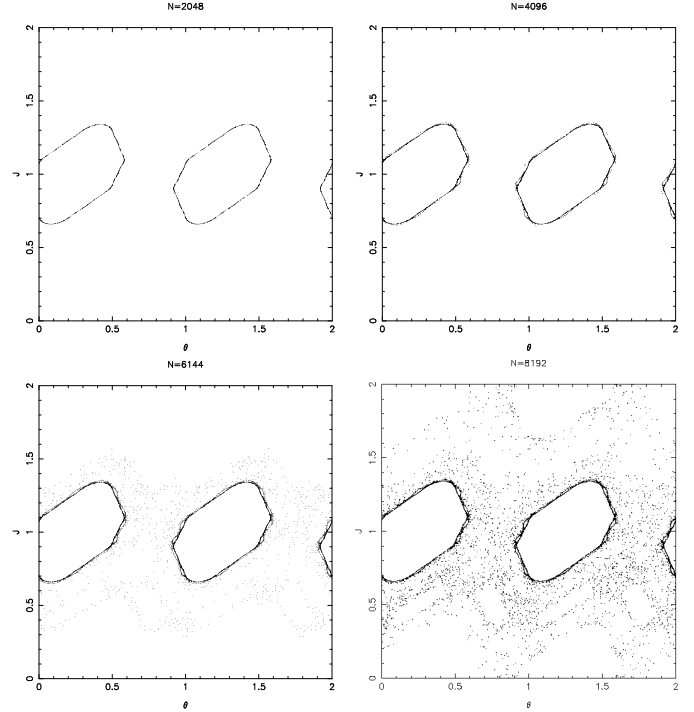


Fig. 1. The successive points of the “sticky” trajectory (starting at $J_0 = \pi$, $\theta_0 = 1.538 \pi$). Upper left, the first 2048 points, upper right the first 4096, down left, the first 6144 and down right, the first 8192. The units in all axes are given as multiples of π

The frequencies covered by the power spectrum are

$$f_j = f_c \frac{j}{M} \quad j = 0..M \quad (6)$$

In the present work we used the so called “Hanning” window. More details on the calculation of the power spectrum can be found in the book by Press et. al. (1992).

As a rule “mixed” methods are expected to perform better in distinguishing between ordered and chaotic trajectories. The reason for that is that time series that are constructed from the geodesic divergence of nearby orbits contain all the various characteristic frequencies that locally affect the motion in the “proper” ratio, i.e. the frequencies corresponding to the different directions (degrees of freedom) are properly weighted. In particular now, as far as our method is concerned, the Power Spectrum Of Divergences (PSOD) of an ordered trajectory is expected to possess only a few “spikes” at specific frequencies. The number of harmonics however depends on the system under consideration as well as on the values of its “control” parameters (see below). In contrast, the PSOD of a chaotic trajectory should appear continuous, due to the random nature of the q_k time series. However, the above considerations lie behind all methods based on time series analysis. What is really important, for the assessment of the new method with respect to the other ones appearing in the literature, is to evaluate (a) its independence from the number of degrees of freedom of the dynamical system, (b) its effectiveness with respect to the

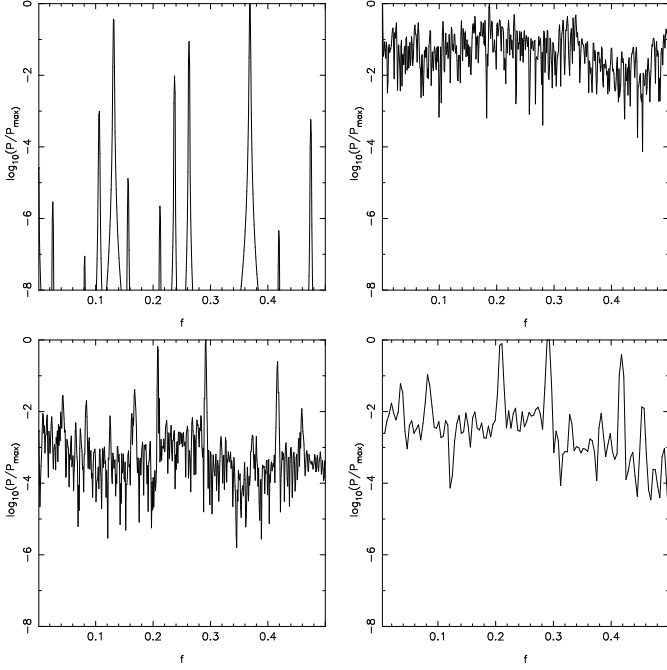


Fig. 2. The PSOD for the three trajectories of the 2-D mapping and for $N=1024$ iterations. Upper left : *map1* trajectory, upper right : *map2* trajectory, down left : *map3* trajectory and down right : *map3* trajectory but now with $N=256$

object of test (single trajectories or distributions of initial conditions covering wide phase space regions) (c) its sensitivity, i.e. the minimum length of the time series, necessary to distinguish a sticky chaotic trajectory from an ordered one and (d) its ability to produce a well-defined measure of chaos (as is the LCN).

3. Evaluation of the method

We proceed in the assessment of the method using three different dynamical systems, namely a 2-D mapping as well as a 2-D and a 3-D Hamiltonian system. In each one we evaluated the nature of a considerable number of trajectories. In the following subsections we present only three or four trajectories per system, which we think that are typical examples of the three different classes of trajectories, i.e. ordered, clearly chaotic and sticky. The amplitudes of the PSOD, in all figures, are normalized so that the highest has the value one, while the frequency is given in cycles per time unit.

3.1. 2-D mapping

We first test the method in the simple 2-D mapping

$$\begin{aligned} J_{i+1} &= J_i + k \cos(2\theta_i) \mod(2\pi) \\ \theta_{i+1} &= \theta_i + J_{i+1} \mod(2\pi) \end{aligned} \quad (7)$$

where the stochasticity parameter k is taken equal to 0.7.

We present here the results of three trajectories, an ordered one (*map1*) starting at $J_0 = \pi$, $\theta_0 = 1.4\pi$, a stochastic one

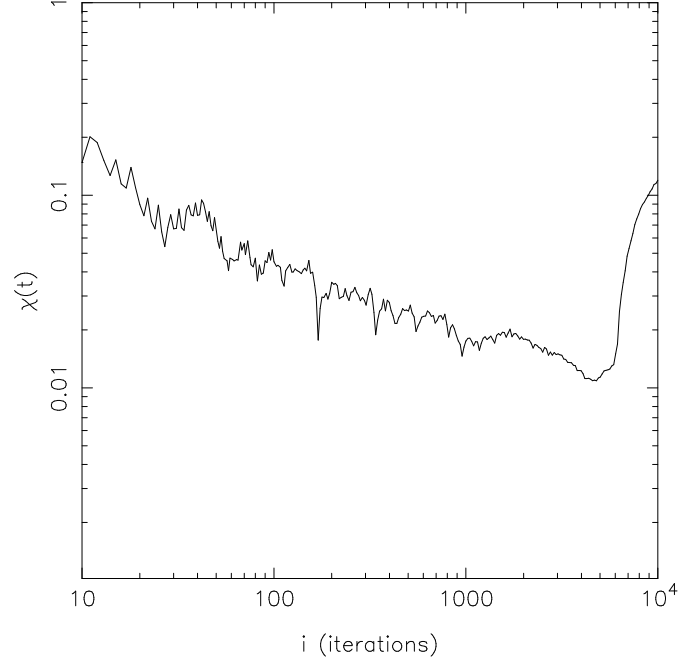


Fig. 3. The evolution of $\chi(t)$ for the sticky trajectory in the 2-D mapping

(*map2*) starting at $J_0 = \pi$, $\theta_0 = 1.5\pi$ and a sticky one (*map3*) starting at $J_0 = \pi$, $\theta_0 = 1.538\pi$. The initial conditions of the third one place it very close to the boundary between the ordered region, surrounding the stable point $J_0 = \pi$, $\theta_0 = 5\pi/4$, and the chaotic sea. Figure 1 shows the consequents (θ, J) of the “sticky” trajectory at various times (iterations). As we can see, for up to 2 048 iterations the trajectory behaves like an ordered one. Around $i = 4\,000$ it starts to present some signs of irregularity and finally, after $i = 6\,000$, the chaotic nature of the trajectory becomes evident. Using our method on these three trajectories, with the length of the q_k time series being $N=1024$ iterations and defining $\Delta t = 1$, we obtain the spectra shown in Fig. 2.

The upper left frame of Fig. 2 is the spectrum of the ordered trajectory. The spectrum consists of some basic frequencies while the “noise” is at a very low level. On the contrary, the spectrum of the chaotic trajectory, in the upper right frame, covers the whole frequency range with comparable amplitudes, i.e. a clearly continuous spectrum. Looking at the spectrum of the “sticky” trajectory (lower left frame), we see a pattern almost the same as that of the chaotic one. Some high-amplitude spikes are evident but the continuum noise level is again very high for the whole frequency range, denoting the stochastic nature of the trajectory. Even with much less iterations ($N=256$ - lower right frame of Fig. 2) we get the same result. The spectrum is less dense, since it has a smaller number of frequencies than before (see eq.(6)), but the basic features are the same. Note that for the LCN, which is the limit of the function

$$\chi(t) = \frac{1}{N \Delta t} \sum_{i=1}^N q_i \quad (8)$$

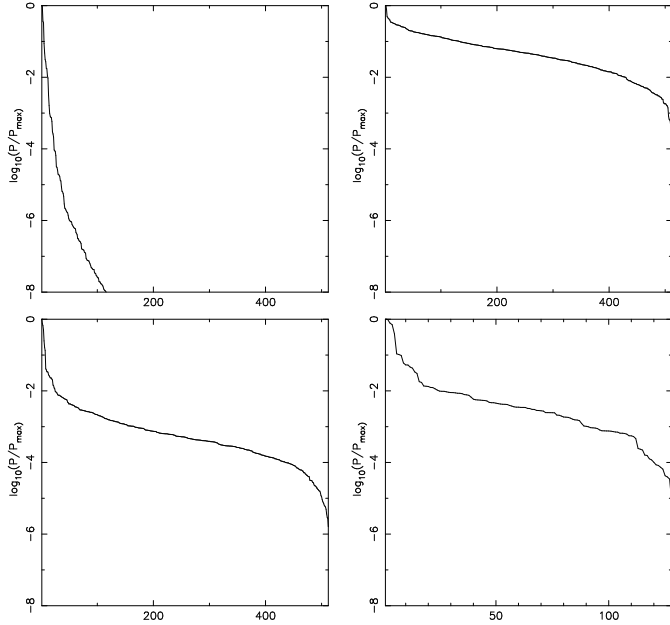


Fig. 4. The PSOD for the three trajectories in the 2-D mapping shown in Fig. 2, the peaks being sorted in descending order of amplitude. The first three frames are for $N=1024$ iterations, while the fourth (down right) is *map3* trajectory with $N=256$ iterations.

as $N \rightarrow \infty$ (see Fig. 3), or the plot of the consequents of the mapping (Fig. 1), we need much more than 1024 iterations in order to decide whether the trajectory is chaotic or not.

3.2. An improved criterion

The above presented results show that it is, indeed, worth to consider the new method as a useful tool in the assessment of the nature, ordered or chaotic, of a trajectory. However the method, as it is, does not entail a *clear and easy to apply* criterion for the classification of a trajectory as ordered or chaotic. Here we try to improve somehow the presentation of the results of our method, in order to propose such a criterion. Note that this new criterion is similar, graphically, to the criterion of the FLI proposed by Froeschlé et al (1997).

If the peaks appearing in the PSOD are plotted in descending order of amplitude, we have a graphical representation of how many strong frequencies the spectrum possesses. Figure 4 shows this representation of the PSOD for the three trajectories studied in the previous sub-section. Ordered trajectories have only a few high amplitude frequencies and the background is formed by peaks whose amplitudes are more than four orders of magnitude smaller than that of the basic frequency. On the other hand the stochastic trajectories possess only a few high-amplitude frequencies and the largest part of the spectrum consists of a “continuum” of frequencies with also considerable amplitude. In this respect one may choose to represent the results by a single number (e.g. the number of peaks up to a certain amplitude), provided that a certain “threshold” for the noise level

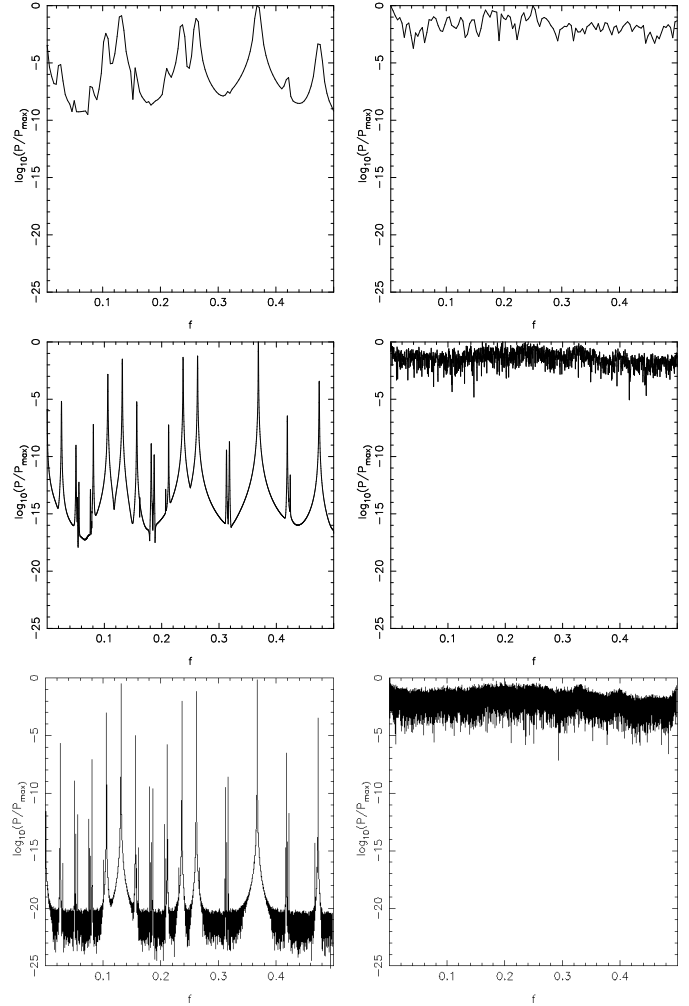


Fig. 5. The PSOD for the regular (left) and the chaotic (right) trajectories in the 2-D mapping with $N=256$ (top), $N=4096$ (middle) and $N=65536$ (bottom).

is chosen (10^{-8} in Fig. 4). This value will, however, depend on the system at study.

3.3. Noise level

Any method of analysis of finite-sample time series is bound to suffer from noise. Thus, even in the PSOD of a regular orbit a certain noise level is expected. This is mainly due to “leakage” of power from the frequency lobes, a side effect of the calculation of the power spectrum using Discrete Fast Fourier Transform methods. When calculating the power spectrum of a “monochromatic” signal, the power contained in its basic frequency “leaks” into neighboring frequencies. The leakage depends on the windowing function used. When a signal possesses two closely spaced frequencies, all frequencies in between these two will also gain considerable amplitudes, due to this phenomenon. If the PSOD of a regular orbit has a large number of basic (strong) frequencies, then this effect can lead us to falsely identify it as chaotic. The problem can be tackled

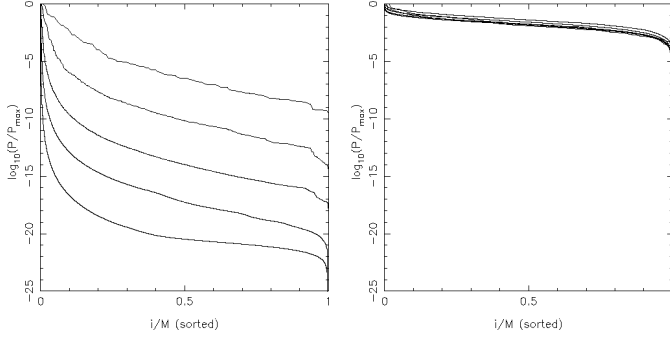


Fig. 6. The sorted PSOD for the regular (left) and the chaotic (right) trajectories in the 2-D mapping for different iteration number, N . Lines from top to bottom correspond to $N=256$, 1024, 4096, 16384 and 65536.

at the cost of taking more points in the sample. In this way, the number of frequencies appearing in the spectrum is increased but the frequency lobes become thinner. Thus, lobe overlapping is reduced and the noise level drops. For chaotic orbits on the other hand, the observed noisy pattern is an inherent property of the spectrum and by increasing the number of points one cannot alter the picture.

The above can be seen in Fig. 5, which shows the PSOD of a regular (left column) and a chaotic trajectory (right column) for three different values of N , i.e. $N=256$ (top), $N=4096$ (middle) and $N=65536$ (bottom). As we see, the noise level in the case of the regular orbit drops significantly when N is increased, while in the case of the chaotic orbit it remains more or less unchanged. In the $N=65536$ case the noise level for the ordered trajectory drops below 10^{-20} , becoming comparable to the accuracy of the FFT calculation (double precision).

This phenomenon is better seen if we use the amplitude-sorted PSOD. Fig. 6 shows the amplitude-sorted PSOD of the regular (left) and chaotic (right) trajectory with $N=256$, 1024, 4096, 16384 and 65536. While the noise level in the PSOD of the ordered trajectory is reduced when N is increased, it remains the same for the chaotic one.

3.4. 2-D Hamiltonian system

We now proceed to test the method in a 2-D Hamiltonian system. We selected the Hamiltonian used by Caranicolas & Vozikis (1987),

$$H = \frac{1}{2} (p_x^2 + p_y^2) + x^4 + y^4 + 2ax^2y^2 = h \quad (9)$$

where the parameter a is taken equal to 2.0 and the energy constant $h = 1.0$.

Again we study three trajectories, one ordered (*ord-2*) starting at $x(0) = 0.5$, one clearly stochastic (*ch-2*) starting at $x(0) = 0.001$ and one “sticky” (*st-2*) which starts at $x(0) = 0.1326$. All three trajectories have also $y(0) = 0$ and $p_x(0) = 0$, while their $p_y(0)$ is given by the energy integral.

Using the PSOD with a renormalization time-step equal to $\Delta t = 1.5$, we find that the spectra of the three test trajec-

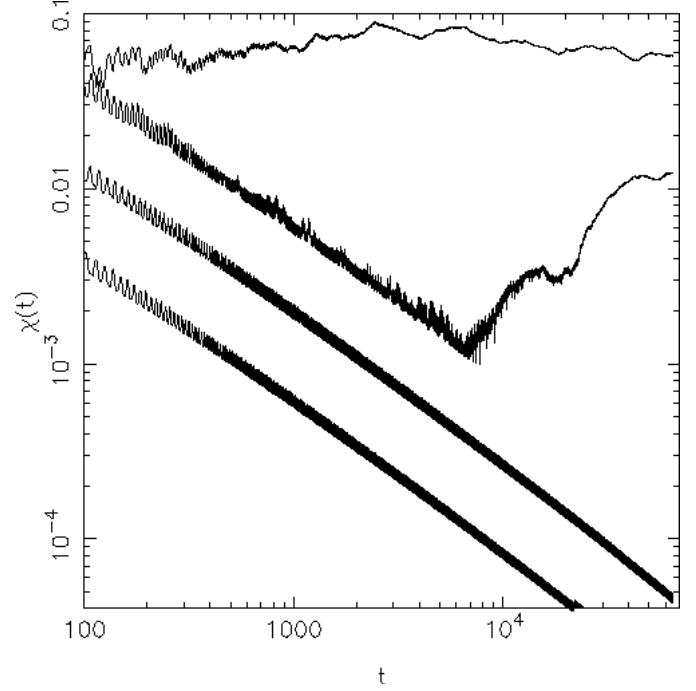


Fig. 7. The evolution of $\chi(t)$ of the four test trajectories in the 2-D Hamiltonian model in the case $a = 2$. The initial positions of the trajectories are given in the text. Note that the $\chi(t)$ curves of the two ordered trajectories have been lowered by one (*ord-2*) and half (*ord-2a*) orders of magnitude in order to be clearly distinguished from the sticky trajectory

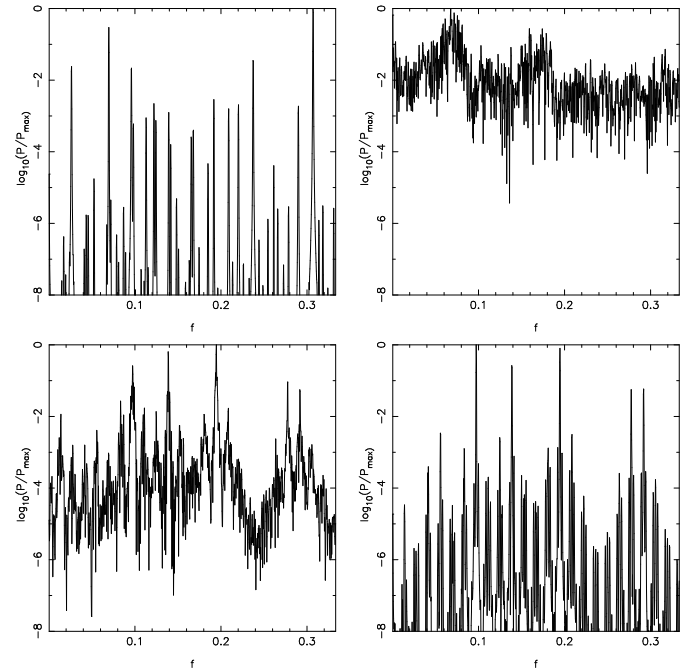


Fig. 8. The PSOD, with $N=2048$, of the four test trajectories in the 2-D Hamiltonian model for $a = 2$. Upper left: the ordered *ord-2*, upper right: the chaotic *ch-2*, lower left: the sticky *st-2* and lower right: the ordered *ord-2a*.

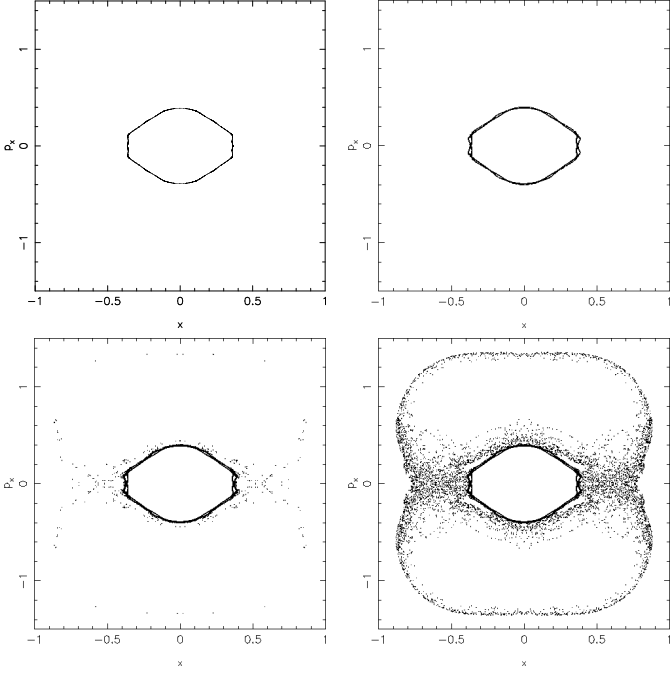


Fig. 9. The surface of section x, \dot{x} of $st-4$ in the 2-D Hamiltonian model. Upper left $t = 3\,000$, upper right $t = 8\,000$, down left $t = 15\,000$, down right $t = 20\,000$

ries present the same properties as those of the corresponding cases of the mapping. In Fig. 8 we see the PSOD of the three test trajectories. The difference between the spectrum of the chaotic trajectory $ch-2$ and that of the ordered trajectory $ord-2$ is again obvious. Moreover, the “sticky” trajectory $st-2$ has a spectrum similar to that of $ch-2$. Note that we have used only 2048 points (corresponding to $t = 3072$) while, if we look at the evolution of the $\chi(t)$ (Fig. 7), the trajectory looks ordered for a time up to $t \approx 7\,000$. The fourth frame (lower right) in Fig. 8 corresponds to another regular orbit ($ord-2a$) that starts at $x = 0.133$, i.e. very close to the sticky trajectory. We see that, although the two trajectories start very close to each other and, at least for the first 3 000 times steps, span approximately the same phase-space region, their PSODs are completely different, clearly revealing the nature of each case.

We decided to test also the case where the parameter a is taken equal to 4.0. As Caranicolas & Vozikis (1987) have shown, the surface of section of this case has a completely different topology from that of the $a = 2$ case. The equipotential curves have negative curvature along the $y = \pm x$ lines. This affects mainly the loop orbits which appear “squared”.

Again we study four trajectories, one ordered ($ord-4$) starting at $x(0) = 0.3$, one clearly chaotic ($ch-4$) starting at $x(0) = 0.7$, one “sticky” ($st-4$) which starts at $x(0) = 0.36282$ and one ordered ($ord-4a$) starting at $x(0) = 0.362$ very near to the sticky one. The surface of section plot for the “sticky” trajectory is shown in Fig. 9 at various times. Figures 10 and 11 present the PSOD and the amplitude-sorted PSOD for these four orbits ($N=4096$). An important characteristic seen in these two figures is the presence of a high number of medium-

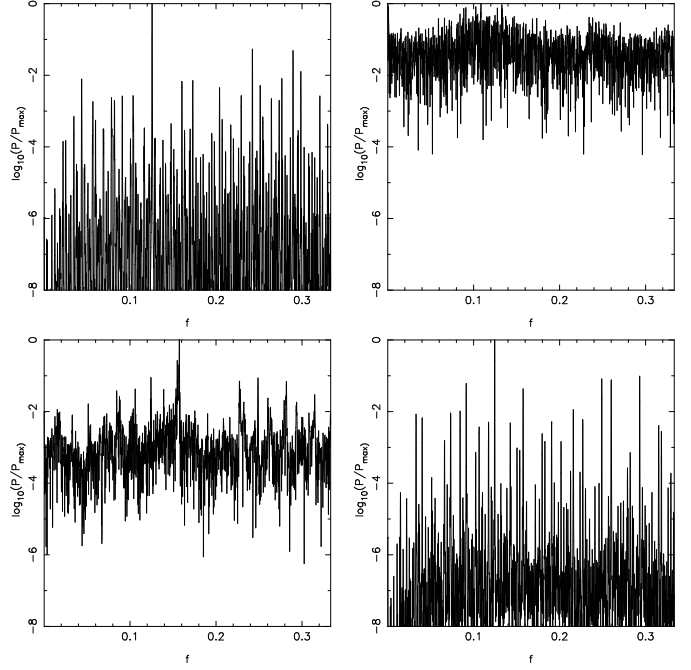


Fig. 10. The PSOD, with $N=4096$, of the four test trajectories in the 2-D Hamiltonian model for $a = 4$. Upper left: the ordered $ord-4$, upper right: the chaotic $ch-4$ and lower left: the sticky $st-4$ and lower right: the ordered $ord-4a$.

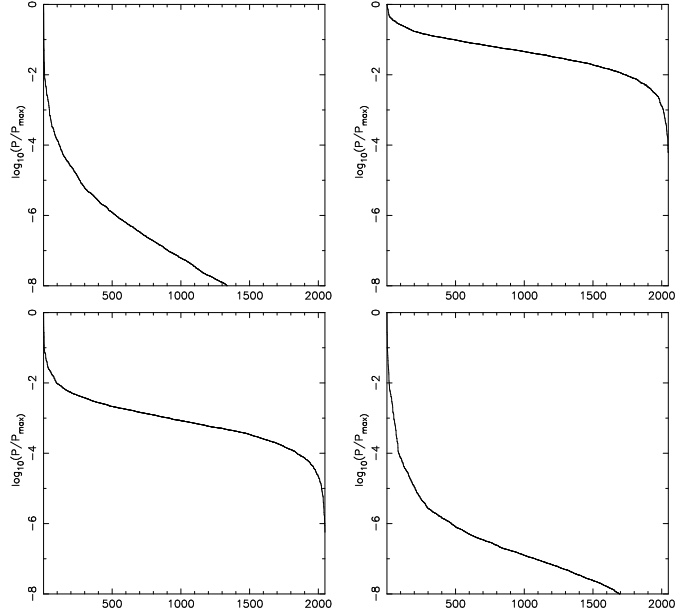


Fig. 11. The sorted PSOD of Fig. 10

amplitude frequencies in the spectra of the regular orbits. However, a distinction between regular and chaotic orbits can still be made. Due to frequency overlapping, discussed in section 3.3, individual frequencies cannot be distinguished at an amplitude level smaller than 10^{-6} . This makes it very difficult to identify a sticky orbit with an amplitude level around $10^{-6} - 10^{-7}$. Nevertheless the noise level of the regular or-

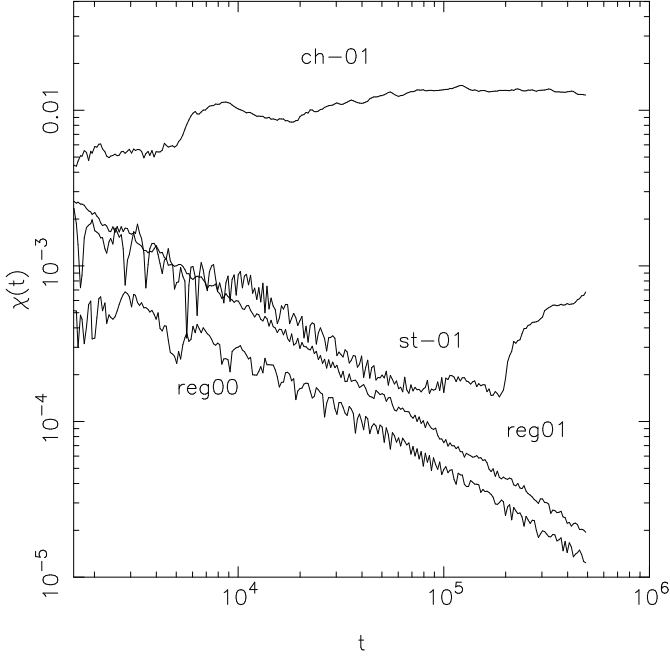


Fig. 12. The evolution of $\chi(t)$ of the four test trajectories in the 3-D Hamiltonian model. The initial positions of the trajectories are given in the text.

bits will be suppressed if we take more points, while for a sticky chaotic orbit it will remain more or less the same.

3.5. 3-D Hamiltonian system

We apply our method to the model Hamiltonian used by Magennat (1982), Contopoulos & Barbanis (1989), Barbanis and Contopoulos (1995), Barbanis (1996), Varvoglis et al. (1997), Barbanis et. al. (1999) and Tsiganis et al. (2000a)

$$H = \frac{1}{2} (p_x^2 + p_y^2 + p_z^2) + \frac{1}{2} (Ax^2 + By^2 + Cz^2) - \epsilon xz^2 - \eta yz^2 = h \quad (10)$$

where the parameters are taken as $A = 0.9$, $B = 0.4$, $C = 0.225$, $\epsilon = 0.560$ and $\eta = 0.20$ and the energy level is $h = 0.00765$

We again test three trajectories, an ordered one (*reg01*) starting at $\bar{x} = 0.01$, $\bar{y} = 0.032$, a chaotic one (*ch-01*) starting at $\bar{x} = 0$, $\bar{y} = 0$ and a sticky one (*st-01*) with initial conditions $\bar{x} = 0.01725$, $\bar{y} = 0.032$, while \bar{z} , p_x , p_y were taken equal to 0 and p_z is calculated from the energy integral. We use the variables \bar{x} , \bar{y} , \bar{z} instead of x , y , z in order to be consistent with the previous publications. The barred variables are defined as $\bar{x} = \sqrt{A}x$, $\bar{y} = \sqrt{B}y$ and $\bar{z} = \sqrt{C}z$.

In 3-D one cannot visualize a surface of section plot, in order to check whether a particular trajectory is ordered or chaotic. Therefore, if one is using the traditional tools, he has to rely on the calculation of LCNs. It should be pointed out that a positive LCN is a proof that the trajectory under study is chaotic, while a monotonically decreasing value of $\chi(t)$ is not

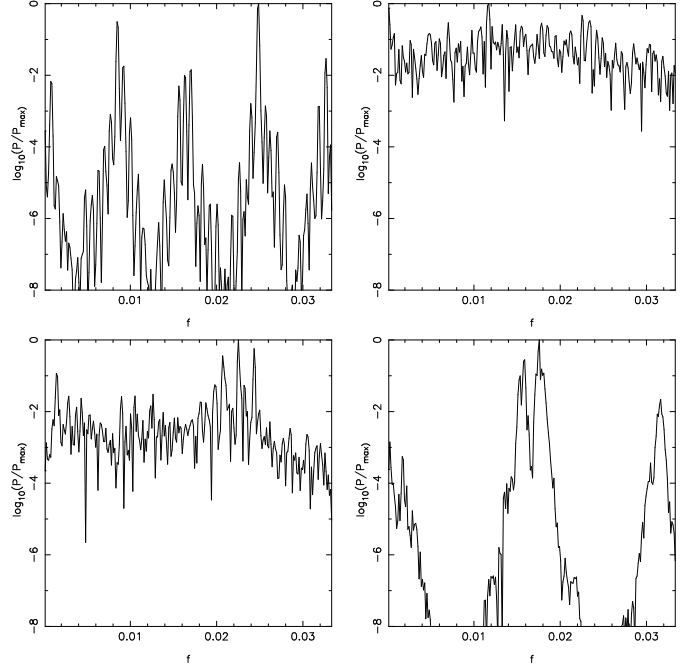


Fig. 13. The PSOD of the four test trajectories in the 3-D Hamiltonian model using 512 points. i.e. 7680 time steps. Upper left the ordered *reg01*, upper right the chaotic *ch-01*, lower left the sticky *st-01* and lower right the ordered *reg00*.

a proof of order, since this behavior could very well originate from “stickiness”. That is why we decided to test one more trajectory (*reg00*) for which we can be almost certain that it is ordered, as it has the same initial position as *reg01* but it belongs to an almost integrable case of the model Hamiltonian, $\epsilon = 0.01$ and $\eta = 0.01$.

Figure 12 shows the calculation of the $\chi(t)$ for the four trajectories. We can clearly see that $\chi(t)$ of *st-01* is decreasing up to $t = 7 \cdot 10^4$ and then begins to saturate to a non-zero LCN value. The stochasticity is even more evident after $t = 2.2 \cdot 10^5$, where we have a “jump” to a higher LCN value.

We calculate the PSOD using $\Delta t = 15$, a value approximately equal to the time interval between two consecutive crossings of the $\bar{x} - \bar{y}$ plane by the trajectory. Figure 13 shows the PSOD of the four trajectories using 512 points, i.e. for $t = 7680$. Note once again that we can decide that the “sticky” trajectory *st-01* is actually stochastic well in advance of the LCN method. The LCN shows the stochastic behaviour of the trajectory only after $t = 70\,000$, while with the PSOD we need a modest $t = 7680$.

4. Comparison with other methods

As we already mentioned in the introduction, three of the most recent methods for distinguishing ordered from chaotic trajectories are the Fast Lyapunov Indicators (FLI) (Froeschlé et al. 1997), the “spectra” of stretching numbers and/or twist angles (Froeschlé et al. 1993, Voglis & Contopoulos 1994, Contopoulos & Voglis 1997) and the “spectral distance” (DSD) (Voglis

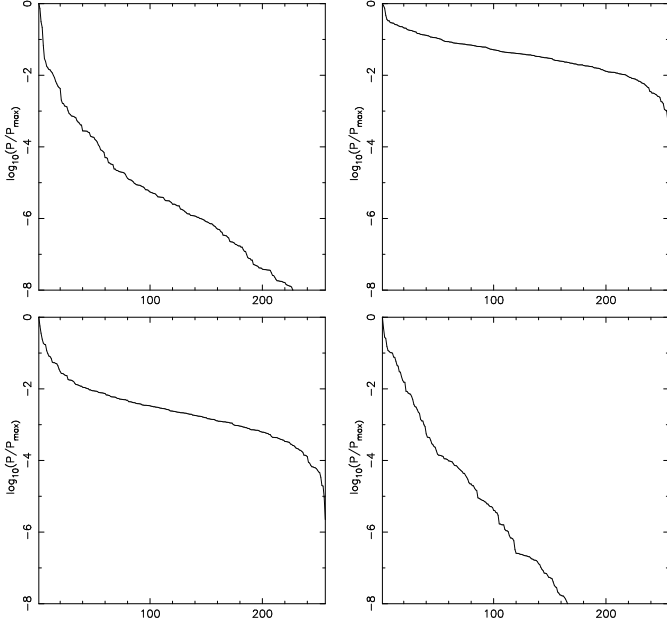


Fig. 14. The PSOD of the four test trajectories in the 3-D Hamiltonian model shown in Fig. 13, the peaks being sorted in descending order of amplitude.

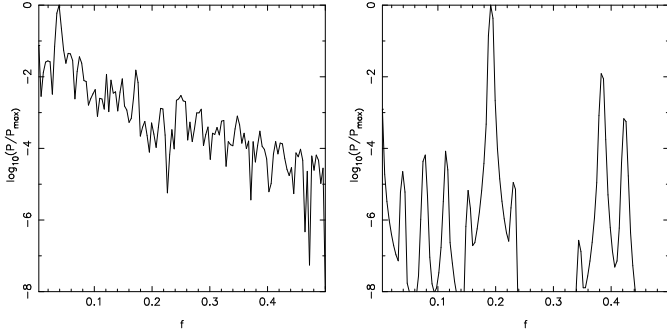


Fig. 15. The PSOD of the two trajectories used by Froeschlé et al. (1997) to test the FLI method. In the left frame is the PSOD of the chaotic trajectory ($x(0) = 0.001, y(0) = 0.001$) and in the right frame is the PSOD of the ordered trajectory ($x(0) = 1, y(0) = 0$).

et al. 1998, 1999). Out of these three methods the fastest ones are the FLI and the DSD methods. In this section we compare the PSOD with the FLI and the DSD methods by applying it to the test models presented in the above mentioned papers. A discussion concerning the spectra of stretching numbers follows.

4.1. Single trajectories

4.1.1. FLI

In the paper by Froeschlé et al. (1997) the authors tested the FLI method on two trajectories of the standard map

$$\begin{aligned} x_{i+1} &= x_i + k \sin(x_i + y_i) \mod(2\pi) \\ y_{i+1} &= x_i + y_i \mod(2\pi) \end{aligned} \quad (11)$$

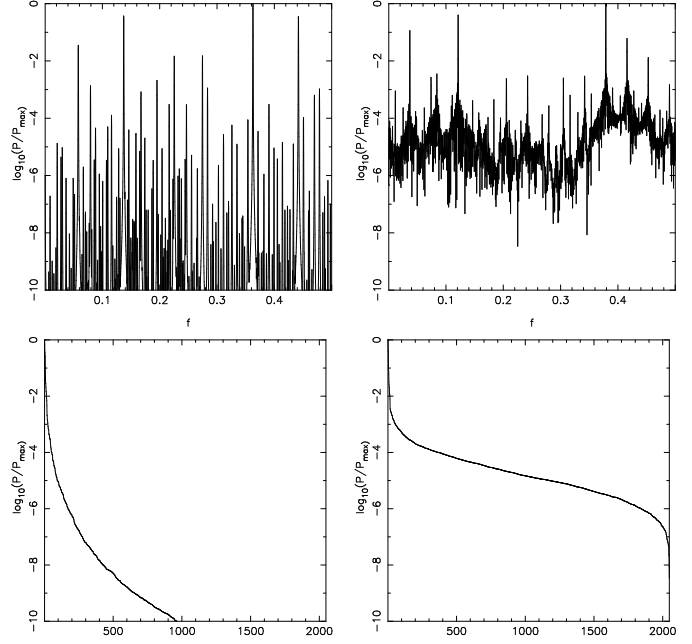


Fig. 16. The PSOD (upper frames) and the sorted PSOD (lower frames) of the two test trajectories (left frames : regular A2, right frames : chaotic A3) in the 4-D mapping for $N=4096$.

with $k = 0.3$; one stochastic starting at $x = 0.001, y = 0.001$ and one ordered starting at $x = 1, y = 0$. They found that for the stochastic trajectory the FLI's drop very quickly down to 10^{-20} (Fig. 2 in their paper - 200 iterations). On the contrary, the function $\chi(t)$ levels only after about 10 000 iterations. For the ordered trajectory the FLI's are slowly decreasing, following $\chi(t)$. In Fig. 15 we present the PSOD's of the stochastic (left frame) and the ordered (right frame) trajectory, calculated using only 256 iterations. It is obvious that the two spectra clearly differentiate between the two types of trajectory.

4.1.2. Spectral distance (the 4D map)

In a recent paper Voglis et al. (1999) proposed, as a tool for the distinction between chaotic and regular orbits in 4D maps, the use of the “spectral distance” D^2 . The method is based on the property that the “spectrum” of *stretching numbers* (as well as that of the *helicity angles*) of a chaotic trajectory is independent of the initial orientation of the deviation vector, while the spectrum of a regular trajectory is not.

The “spectral distance” D^2 is a norm defined as

$$D^2 = \sum_q [S_1(q) - S_2(q)]^2 \quad (12)$$

where the summation is for all q 's and S_1, S_2 are two spectra of the same orbit but with two different initial deviation vectors.

Voglis et al. (1999) applied their method to a 4-D mapping consisting of two coupled 2-D standard maps, i.e.

$$\begin{aligned} x'_1 &= x_1 + x'_2 \\ x'_2 &= x_2 + \frac{k}{2\pi} \sin(2\pi x_1) - \frac{\beta}{\pi} \sin(2\pi(x_1 - x_3)) \end{aligned} \quad (13)$$

$$\begin{aligned} x'_3 &= x_3 + x'_4 \\ x'_4 &= x_4 + \frac{k}{2\pi} \sin(2\pi x_3) - \frac{\beta}{\pi} \sin(2\pi(x_3 - x_1)) \end{aligned}$$

where the x_i 's are defined in the interval $[0,1)$ (i.e.mod1).

We chose to test our method upon the two most interesting cases shown in Voglis et al. (1999), namely trajectories A2 and A3, in their notation. The A2 case has initial conditions $(x_1, x_2, x_3, x_4) = (0.55, 0.1, 0.62, 0.2)$, $\beta = 0.1$ and is a regular orbit, while the A3 case has the same initial x_i 's, $\beta = 0.3051$ and is a chaotic orbit but with a very low value of LCN (around $4 \cdot 10^{-7}$).

Fig.16 shows the PSOD of the two test trajectories. The left panel corresponds to the regular orbit (A2) and the right panel corresponds to the chaotic one (A3). The spectra were calculated using 4096 iterations for each orbit. The distinction between the regular and the chaotic orbits is apparent. Note that our method gave the same result as the D^2 method with almost the same computational effort. Of course, both methods are much faster than the traditional LCN method.

4.1.3. “Spectrum” of stretching numbers

The “spectrum” of stretching numbers, $S(q)$, (Froeschlé et al. 1993, Voglis & Contopoulos 1994, Contopoulos & Voglis 1997, Dvorak et al. 1998) is a method also based on the divergence of nearby trajectories. It consists of the calculation of the probability density of q_k (eq.(1)), i.e.

$$S(q) = \frac{\Delta N(q)}{N dq} \quad (14)$$

where $\Delta N(q)$ is the number of q_k with values between q and $q + dq$. A quasi-periodic trajectory, which lies very close to a periodic trajectory, has a “U” shaped distribution of stretching numbers which is also symmetric around $q = 0$ (Contopoulos et al. 1997). As we move away from the periodic trajectory, this symmetry is destroyed (Caranicolas & Vozikis 1999) and the spectrum starts to develop a greater number of maxima. On the other hand if the trajectory is chaotic, the spectra have different shapes and are not symmetric at all. It should be pointed out, however, that, in order to obtain a well defined spectrum, one needs to account for a large number of iterations (typically $N = 10^5$ or more). Therefore, we did not attempt to compare this method to our own.

4.2. Sets of trajectories

In order to circumvent the problem of calculating a trajectory for long times, Contopoulos and Voglis (1997) proposed the use of the average value of q ,

$$\langle q \rangle = \frac{1}{N} \sum_{k=1}^N q_k \quad (15)$$

If we keep N small, we can scan a wide area of initial conditions and map its dynamical behavior. Trajectories in chaotic domains will have $\langle q \rangle$ scattered around the value of the

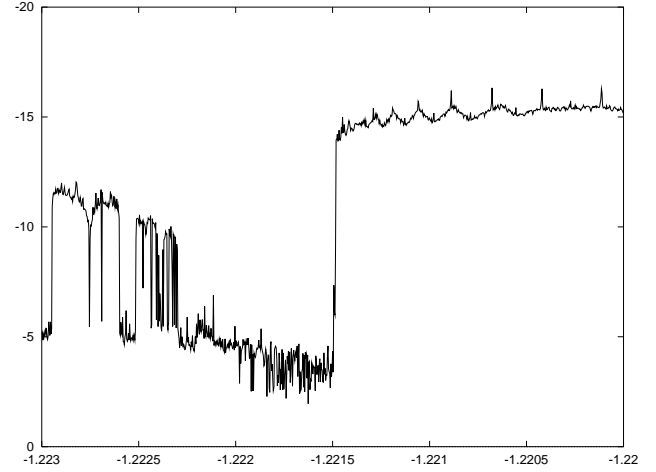


Fig. 17. The logarithm of the average amplitude of PSOD in a cross section of 1000 trajectories near the 1/6 resonance in the standard map of eq.(6)

LCN of this domain, while trajectories in the ordered domain will have $\langle q \rangle$ near zero. The method is very fast in distinguishing between ordered and chaotic domains. Fig. 9 of Contopoulos & Voglis (1997) is a very good example of the results obtained by this method with only 10 iterations.

However, although the method is very good in scanning wide areas of phase space for locating islands of order, it cannot give reliable results with so few iterations for a particular trajectory. In the case of stochastic trajectories, $\langle q \rangle$ for $N = 10$ varies so much, that it may yield a number as small as the one given for ordered trajectories. The situation is even worse in the case of sticky trajectories (i.e. in the borders of islands). In order to decide on the character of such trajectories one needs considerably longer calculations.

Froeschlé & Lega (1998) tested the FLI method along with the method of twist angles (Contopoulos & Voglis 1997), the frequency map analysis method (Laskar et al. 1992, Laskar 1993) and the sup-map method (Laskar 1990, Froeschlé & Lega 1996). Figs. 8a-d of their paper shows the results of the four methods on a cross section of 1 000 trajectories near the hyperbolic point of the 1/6 resonance of the standard map (Eq. 11) with $k = -1.3$. For the FLI method they used 2 000 iterations while for the other three methods 20 000 iterations. In order to produce unambiguous results, the trajectories in this test are classified as ordered or chaotic by an appropriately selected number/indicator. For the FLI method the authors have used as an indicator the time necessary for the FLI to reach a value lower than 10^{-10} .

In order to compare our method with these results we need also an one-number indicator derived from the PSOD. As such we have selected here the average value of $\langle P/P_{max} \rangle$. The averaging is performed not over all values but by ignoring the highest 1/6th and the lowest 1/6th of the amplitudes, the former being probably due to periodicities in sticky trajectories and the latter probably coming from numerical errors in the integration and the calculation of the power spectrum. Fig. 17 shows the

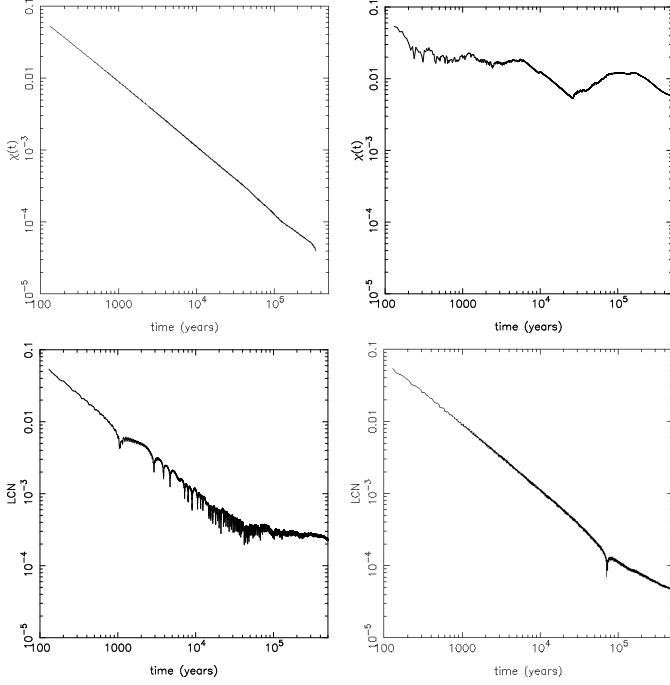


Fig. 18. The evolution of $\chi(t)$ of the trajectories of four asteroids. Upper left, an ordered trajectory with initial $a = 3$, $e = 0$; Upper right a highly stochastic trajectory with $a = 4$, $e = 0.2$; Lower left, a stochastic trajectory with stickiness and with initial $a = 3.64$, $e = 0.08$; Lower right, another sticky orbit with initial $a = 3.63$, $e = 0.08$

same cross section with Fig. 8a-d of Froeschlé & Lega (1998), using the above indicator taken after 8 192 iterations. As we can see it gives essentially the same information as the other four methods. Note that the y-axis in Fig. 17 is inverted for easier comparison with Fig. 8a-d of Froeschlé & Lega (1998).

5. Application to asteroidal motion

As an application of our method to a problem of physical importance, we shall use it in order to assess the chaotic or not nature of asteroidal trajectories. We use a simplified model of the solar system, namely the planar restricted three body problem where the Sun and Jupiter move on elliptic trajectories around their center of mass and an asteroid of infinitesimal mass moves in the gravitational field of the two bodies. We calculate the PSOD and the LCN using as renormalization time, Δt , the period of Jupiter, i.e. $\Delta t = T_J \simeq 11.86$ years.

Fig. 18 shows the $\chi(t)$ of the four trajectories tested. The upper left frame belongs to an ordered trajectory starting with semi-major axis $a = 3$ and eccentricity $e = 0$, the upper right to a stochastic trajectory with initial elements $a = 4$, $e = 0.2$. The other two frames correspond to trajectories with initial $a = 3.64$, $e = 0.08$ (lower left) and $a = 3.63$, $e = 0.08$ (lower right) representing “clones” of the asteroid 522 - Helga, which is a well-known example of “stable chaos” (Milani & Nobili 1992).

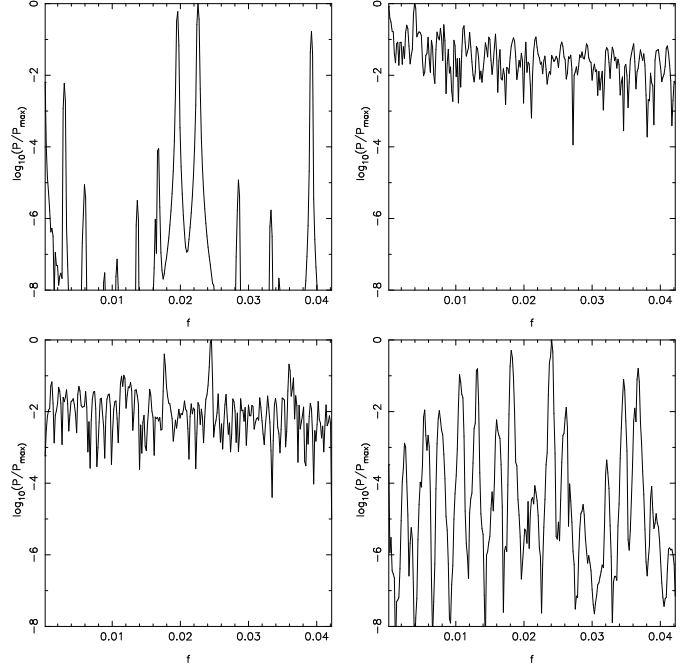


Fig. 19. The PSOD of the four asteroidal trajectories with $N=512$, i.e. 6062 years

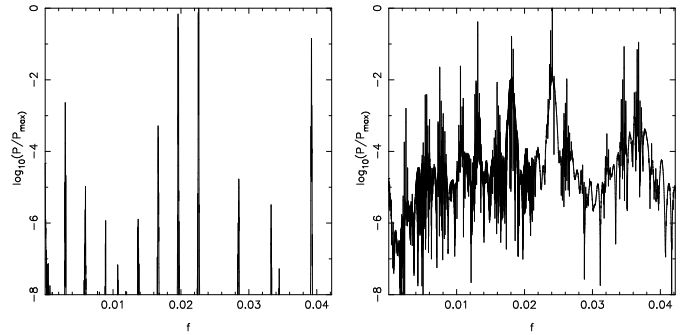


Fig. 20. The PSOD, with $N=8192$, of the ordered asteroidal trajectory (left) and the chaotic Helga clone with $a = 3.63$, $e = 0.08$ (right)

The PSOD of the four trajectories ($N=512$) is shown in Fig. 19. As we can see, a few Jovian periods are sufficient to decide if the motion of a particular asteroid is stochastic or ordered. In the case of the Helga clone with $a = 3.64$ (lower left of Fig. 19) the PSOD shows clearly a chaotic nature after only 512 Jovian periods i.e. 6 072 years, while even a rough calculation of the LCN needs at least 10^5 years (see lower right frame of Fig. 18). The PSOD of the $a = 3.63$ Helga clone is rather peculiar. Although it differs from that of the ordered orbit (upper left), it is not clearly chaotic, unlike the PSOD of the other Helga clone (lower left). Nevertheless, if we take more points in our time series the chaotic nature of the orbit becomes apparent, as we can see in Fig. 20. However, the spectrum can still be described as having a strong quasi-periodic component, something which is related to the peculiar dynamical nature of this orbit as discussed in Tsiganis et al. (2000b).

6. Conclusions – Discussion

In the present paper we propose an alternative tool, which we call PSOD, for the characterization of the chaotic or not nature of trajectories in conservative dynamical systems. The method is based on the frequency analysis of a time series, constructed by successive records of the amplitude of the deviation vector of nearby trajectories. As discussed in Section 2, such a “mixed”¹ method is expected to have certain advantages. The reason is that the power spectrum of such a time series will contain all the characteristic frequencies of the motion in a properly “weighted” ratio.

The basic characteristic of the PSOD, seen in all three test cases (a 2-D mapping, a 2-D and a 3-D Hamiltonian system), is that

- for ordered trajectories the spectrum possesses only a few high-amplitude peaks, the exact number of which depends not only on the system but also on the particular orbit. Of course a small amplitude noise level, due to the numerical procedure, is superimposed on the spectrum, which diminishes as the length of the time series is increased;
- for chaotic trajectories the spectrum has a noisy pattern. For weakly chaotic orbits a few high-amplitude peaks are also present. Increasing the length of the time series, the spectrum tends to a white noise spectrum which remains practically unchanged for any (large enough) number of points (see Figs. 5 and 6).

Like most methods existing in the literature, it seems that the method performs better for maps than for flows. However, the results found for the three Hamiltonian flows tested (including the three-body problem) show that the method can be applied to any system, no matter how many degrees of freedom are involved. We believe that the results may be significantly improved for flows, provided that proper analysis concerning the renormalization time is conducted. The difference between maps and flows is that, in the former case, isochronous records of dynamical quantities also mean studying the system on a surface of section. This is not the case for flows and, thus, a more refined analysis on how to select a proper renormalization time has to be made.

We have shown that the sensitivity of the PSOD in testing single trajectories in maps is comparable to the FLI and the DSD methods. This also makes the PSOD an efficient tool for scanning wide areas of the phase space (see Section 4). For such purposes one would like to have an one-number indicator for measuring chaos. The only uniquely defined measure of chaos is of course the LCN. Any other indicator should be in a one-to-one correspondence with the LCN, in order to give the same information. There is no guarantee that such an indicator can be based on the frequency content of the PSOD, as chaotic orbits with similar LCNs may have a different frequency distribution. Further analysis of the properties of the PSOD has to

be performed in order to decide whether such an indicator can be found.

Acknowledgements. The authors would like to acknowledge the constructive comments of the anonymous referee.

References

- Barbanis, B., 1996, In: Proceedings of the 2nd Hellenic Astronomical Conference, Contadakis M.E., Hadjidemetriou J.D., Mavridis L.N., Seiradakis J.H. (eds.), P. Ziti & Co, Thessaloniki, p. 520-525
- Barbanis, B., Contopoulos, G., 1995, *A&A*, 294, 33
- Barbanis, B., Varvoglis, H., Vozikis, Ch., 1999, *A&A*, 344, 879
- Benettin, G., Galgani, L., Strelcyn J.M., 1976, *Phys. Rev. A*, 14, 2338
- Caranicolas, N., Vozikis, Ch., 1987, *Cel. Mech.*, 40, 35
- Caranicolas, N., Vozikis, Ch., 1999, *A&A*, 349, 70
- Contopoulos, G., 1966, In: *Les Nouvelles Méthodes de la Dynamique Stellaire*, Nahon, F. & Hénon, M. (eds.)
- Contopoulos, G., Barbanis, B., 1989, *A&A*, 222, 329
- Contopoulos, G., Voglis, N., 1997, *A&A*, 317, 73
- Contopoulos, G., Voglis, N., Efthymiopoulos, C., Froeschlé, C., Gonzi, R., Lega, E., Dvorak, R., Lohinger, E., 1997, *Cel. Mech. Dyn. Astron.*, 67, 293
- Dvorak, R., Contopoulos, G., Efthymiopoulos, Ch., Voglis, N., 1998, *Planet. Space Sci.*, 46, 1567
- Froeschlé, C., 1984, *Cel. Mech.*, 34, 95
- Froeschlé, C., Lega, E., 1996, *Cel. Mech. Dyn. Astron.*, 64, 21
- Froeschlé, C., Lega, E., 1998, *A&A*, 334, 355
- Froeschlé, C., Froeschlé, Ch., Lohinger, E., 1993, *Cel. Mech. Dyn. Astron.*, 51, 135
- Froeschlé, C., Lega, E. and Gonzi, R., 1997, *Cel. Mech. Dyn. Astron.*, 67, 41
- Hénon M. and Heiles C., 1964, *Astron. J.*, 69, 73
- Laskar, J., 1990, *Icarus*, 88, 266
- Laskar, J., 1993, *Physica D*, 67, 257
- Laskar, J., Froeschlé, C., Celletti, A., 1992, *Physica D*, 56, 253
- Lega, E., Froeschlé, C., 1996, *Physica D*, 95, 97
- Lohinger, E. and Froeschlé C., 1993, *Cel. Mech. Dyn. Astron.*, 57, 369
- Magnenat, P., 1982, *Cel. Mech.*, 28, 319
- Milani A. and Nobili A., 1992, *Nature*, 357, 569
- Press W. H., Teukolsky S. A., Vetterling W. T. and Flannery B. P., 1992, *Numerical Recipes in Fortran – The Art of Scientific Computing* 2nd edn (Cambridge: Cambridge University Press)
- Tsiganis K., Anastasiadis A. and Varvoglis H., 2000a, *Chaos Solit. & Fract.* (in press)
- Tsiganis K., Varvoglis H. and Hadjidemetriou J.D., 2000b, *Icarus* (in press)
- Varvoglis, H., Vozikis, Ch., Barbanis, B. 1997, In: *The Dynamical Behaviour of Our Planetary System*, Henrard J., Dvorak R. (eds.), Kluwer, Dordrecht
- Voyatzis, G., Ichtiaoglou, S., 1992, *J. Phys. A*, 25, 5931
- Voglis, N., Contopoulos, G., 1994, *J. Phys. A*, 27, 4899
- Voglis, N., Contopoulos, G., Efthymiopoulos, C., 1998, *Phys. Rev. E*, 57, 372
- Voglis, N., Contopoulos, G., Efthymiopoulos, C., 1999, *Cel. Mech. Dyn. Astron.*, 73, 211
- Voglis, N., Efthymiopoulos, C., 1998, *J. Phys.*, A31, 2913

¹ Since the method uses both the deviation vectors and frequency analysis it may be classified as “mixed”